Noninvasive *In Vivo* Imaging to Evaluate Immune Responses and Antimicrobial Therapy against *Staphylococcus aureus* and USA300 MRSA Skin Infections

John S. Cho[1], Jamie Zussman[1], Niles P. Donegan[2], Romela Irene Ramos[1], Nairy C. Garcia[1], Daniel Z. Uslan[3], Yoichiro Iwakura[4], Scott I. Simon[5], Ambrose L. Cheung[2], Robert L. Modlin[1,6], Jenny Kim[1,7] and Lloyd S. Miller[1]

Staphylococcus aureus skin infections represent a significant public health threat because of the emergence of antibiotic-resistant strains such as methicillin-resistant *S. aureus* (MRSA). As greater understanding of protective immune responses and more effective antimicrobial therapies are needed, a *S. aureus* skin wound infection model was developed in which full-thickness scalpel cuts on the backs of mice were infected with a bioluminescent *S. aureus* (methicillin sensitive) or USA300 community-acquired MRSA strain and *in vivo* imaging was used to noninvasively monitor the bacterial burden. In addition, the infection-induced inflammatory response was quantified using *in vivo* fluorescence imaging of LysEGFP mice. Using this model, we found that both IL-1α and IL-1β contributed to host defense during a wound infection, whereas IL-1β was more critical during an intradermal *S. aureus* infection. Furthermore, treatment of a USA300 MRSA skin infection with retapamulin ointment resulted in up to 85-fold reduction in bacterial burden and a 53% decrease in infection-induced inflammation. In contrast, mupirocin ointment had minimal clinical activity against this USA300 strain, resulting in only a 2-fold reduction in bacterial burden. Taken together, this *S. aureus* wound infection model provides a valuable preclinical screening method to investigate cutaneous immune responses and the efficacy of topical antimicrobial therapies.

Journal of Investigative Dermatology (2011) **131,** 907–915; doi:10.1038/jid.2010.417; published online 30 December 2010

INTRODUCTION

Staphylococcus aureus is the most common cause of skin and soft-tissue infections, such as impetigo, cellulitis, folliculitis/furunculosis, and abscesses (McCaig *et al.*, 2006; Moran *et al.*, 2006). These infections have become a significant public health problem as they result in over 11 million outpatient and emergency room visits and ~500,000 hospitalizations per year in the United States (McCaig *et al.*, 2006). Furthermore, the treatment of *S. aureus* infections has been complicated by the widespread emergence of antibiotic-resistant strains such as methicillin-resistant *Staphylococcus aureus* (MRSA) (Boucher and Corey, 2008; Deleo and Chambers, 2009).

Systemic antibiotic treatment is frequently required to treat *S. aureus* skin infections, especially in cases of community-acquired MRSA (CA-MRSA) infections. One strain, USA300, is responsible for >90% of all CA-MRSA skin and soft-tissue infections in the United States (King *et al.*, 2006; Jones *et al.*, 2007; Tenover and Goering, 2009). USA300 can cause serious and necrotizing skin infections, which are likely because of the expression of cytolytic toxins such as PVL (Panton–Valentine leukocidin), α-toxin and other cytolytic toxins (Wang *et al.*, 2007; David and Daum, 2010; Kennedy *et al.*, 2010).

In addition to systemic antibiotics, topical antibiotic therapy can have an important adjunctive role in the treatment of superficial *S. aureus* skin infections, such as impetigo, infected lacerations, and in areas with poor blood

[1]*Division of Dermatology, David Geffen School of Medicine at UCLA, Los Angeles, California, USA;* [2]*Department of Microbiology and Immunology, Dartmouth Medical School, Hanover, New Hampshire, USA;* [3]*Division of Infectious Diseases, David Geffen School of Medicine at UCLA, Los Angeles, California, USA;* [4]*Center for Experimental Medicine, Institute of Medical Science, University of Tokyo, Tokyo, Japan;* [5]*Department of Biomedical Engineering, University of California, Davis, Davis, California, USA;* [6]*Department of Microbiology, Immunology and Molecular Genetics, David Geffen School of Medicine at UCLA, Los Angeles, California, USA and* [7]*Department of Dermatology, Greater Los Angeles Healthcare System Veterans Affairs, Los Angeles, California, USA*

Correspondence: Lloyd S. Miller, Division of Dermatology, University of California, Los Angeles (UCLA), 52-121 Center for Health Sciences, 10833 Le Conte Avenue, Los Angeles, California 90095, USA.
E-mail: lloydmiller@mednet.ucla.edu

Abbreviations: CA-MRSA, community-acquired MRSA; CFU, colony-forming unit; EGFP, enhanced green fluorescence protein; MRSA, methicillin-resistant Staphylococcus aureus*; PVL, Panton–Valentine leukocidin*

Received 30 June 2010; revised 9 November 2010; accepted 24 November 2010; published online 30 December 2010

supply (i.e., diabetic foot ulcers) as well as in the prevention of postsurgical wound infections (Daum, 2007). Furthermore, topical antibiotics can be used alone for uncomplicated superficial skin infections such as impetigo and infected lacerations, as a higher local concentration of the antibiotic reaches the site of infection and reduces the potential for systemic side effects (Elston, 2007). Mupirocin is the most commonly used prescription-strength topical antibiotic to treat *S. aureus* skin infections (Daum, 2007). In addition, mupirocin is frequently used for decolonization of *S. aureus* and MRSA nasal carriage (Bode *et al.*, 2010). However, *S. aureus* strains with low- and high-level mupirocin resistance have been reported, which contributes to treatment failures (Thomas *et al.*, 2010). Retapamulin is a newer topical antibiotic agent, which has been shown to exhibit potent antibacterial activity against *S. aureus in vitro* and *in vivo* (Yang and Keam, 2008). However, the efficacy of topical retapamulin against an important CA-MRSA strain, such as USA300, has not been well characterized.

Because of this rapidly emerging epidemic and the growing problem of antibiotic resistance, there is a great need for new antibiotic therapies as well as an increased understanding of protective immune responses to help design immune-based therapeutic strategies. Although human skin equivalent culture systems can be used to monitor bacterial colonization and infection *in vitro* (Holland *et al.*, 2008), a preclinical *in vivo* animal model system is required by the FDA (Food and Drug Administration) to determine the efficacy of new antimicrobial treatments before more extensive studies in larger animals or human subjects. Previous animal models to evaluate topical treatment of superficial *S. aureus* infections include a burned skin model (Rode *et al.*, 1988; Heggers *et al.*, 1989), a skin surgical/suture wound (McRipley and Whitney, 1976; Rittenhouse *et al.*, 2006), and a tape-stripping model (Kugelberg *et al.*, 2005; Hahn *et al.*, 2009). In each of these models, euthanasia is required to determine the *ex vivo* bacterial burden using colony counts, and consequently, large numbers of animals are required to determine treatment efficacy. In this study, we set out to develop a *S. aureus* skin infection model utilizing advanced techniques of *in vivo* imaging to noninvasively and longitudinally monitor the bacterial burden and infection-induced inflammation without the need for euthanasia.

RESULTS

In vivo bioluminescence imaging to measure bacterial burden

To model a *S. aureus* skin wound infection, scalpel cuts on the backs of mice were inoculated with a bioluminescent *S. aureus* strain (SH1000). The *in vivo* bacterial burden was determined by measuring the *S. aureus* bioluminescence signals in anesthetized mice (Xenogen IVIS; Caliper Life Sciences, Hopkinton, MA). To determine the optimal bacterial inoculum that produced a consistent skin wound infection, increasing inocula of *S. aureus* (2×10^5, 2×10^6, and 2×10^7 colony-forming units (CFUs) per 10 μl) or no bacterial inoculation (none) were evaluated (Figure 1). 2×10^7 CFUs induced the largest lesions and 2×10^6 CFUs induced intermediate lesion sizes, which were statistically greater than those of uninfected mice (Figure 1a and b). In contrast, 2×10^5 CFUs induced lesions virtually identical to those of uninfected mice. Similarly, 2×10^7 CFUs induced higher bioluminescent signals than 2×10^6 CFUs, but the signals of both inocula decreased at a similar rate (Figure 1c and d). 2×10^5 CFUs resulted in bioluminescent signals that increased on day 1 but decreased on subsequent days to levels below the bioluminescent signals of the other inocula. It is noteworthy that all three inocula had bioluminescent signals that were statistically greater than the background bioluminescence signals (none). As our goal was to produce a *S. aureus* skin wound infection that induced relatively small lesion sizes and bioluminescence signals that were greater than the uninfected scalpel wounds, the intermediate inoculum of 2×10^6 CFUs of *S. aureus* was used in all subsequent experiments.

To confirm that the *in vivo* bioluminescence signals accurately represented the bacterial burden *in vivo*, colony counts were performed on skin biopsies harvested on day 1 from the infected skin lesions (Figure 2). The *ex vivo* bacterial burden of mice inoculated with 2×10^5, 2×10^6, and 2×10^7 CFUs (Figure 2a and b) highly correlated with the corresponding *in vivo* bioluminescence signals (correlation coefficient: $R^2 = 0.9853$; Figure 2c). These data demonstrate that *in vivo* bioluminescence imaging of a *S. aureus* skin wound infection provides a noninvasive and accurate measurement of the *in vivo* bacterial burden.

In vivo fluorescence imaging to measure the infection-induced inflammation

Neutrophil recruitment to the site of infection is required for an effective immune response against *S. aureus* (Verdrengh and Tarkowski, 1997; Molne *et al.*, 2000). To determine the degree of neutrophil recruitment, histological analysis is commonly used. At day 1, skin wounds of mice inoculated with *S. aureus* developed large neutrophilic abscesses observed in both hematoxylin and eosin (H&E)-labeled and anti-Gr-1 mAb (neutrophil marker)-labeled sections compared with control mice that were wounded but not infected with *S. aureus* (Figure 3a). In addition, *S. aureus* bacteria could be detected within the abscess by Gram stain. However, the measurement of neutrophil abscess formation by histology is a nonparametric measurement and requires euthanasia to obtain skin specimens. To noninvasively quantify the inflammatory response, *in vivo* fluorescence imaging of LysEGFP mice, which possess green fluorescent neutrophils, was used (Faust *et al.*, 2000). By combining the use of bioluminescent *S. aureus* and LysEGFP mice, both bacterial burden and neutrophil infiltration (Kim *et al.*, 2008) could be simultaneously measured by sequential *in vivo* bioluminescence and fluorescence imaging (Figure 3b–e). Similar to C57BL/6 mice in Figure 1, *S. aureus*-inoculated LysEGFP mice developed bioluminescence signals that decreased over the course of the infection and were detectable over the background signals of control uninfected mice (Figure 3b and d). In addition, the *S. aureus*-infected LysEGFP mice had significantly greater enhanced green fluorescent protein (EGFP)-neutrophil fluorescent signals

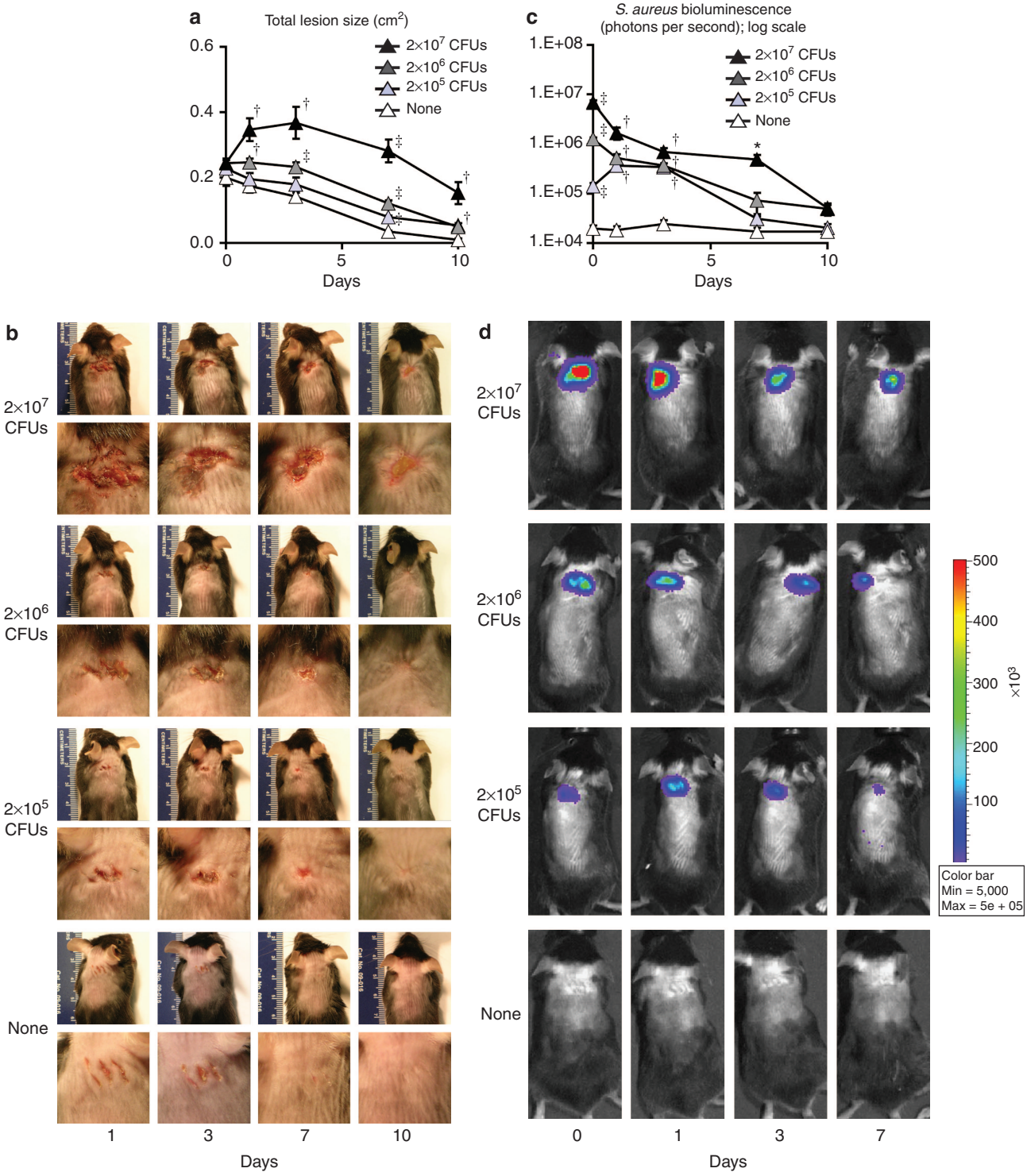

Figure 1. Mouse model of *Staphylococcus aureus* skin wound infection. Three 8-mm in length, parallel, full-thickness scalpel wounds on the backs of mice were inoculated with 2×10^5, 2×10^6, or 2×10^7 colony-forming units (CFUs) per 10 µl of *S. aureus* or no bacteria (none) ($n = 12$ mice per group). (**a**) Mean total lesion size (cm^2) ± SEM. (**b**) Representative photographs of the lesions of the entire dorsal back (upper panels) and close-up photographs of the lesions (lower panels) are shown. (**c**) Bacterial counts as measured by *in vivo S. aureus* bioluminescence (mean total flux (photons per second) ± SEM) (logarithmic scale). (**d**) Representative *in vivo S. aureus* bioluminescence on a color scale overlaid on top of a grayscale image of mice. $^*P<0.05$; $^\dagger P<0.01$; $^\ddagger P<0.001$, *S. aureus*-infected mice versus none (Student's *t*-test).

compared with uninfected control mice at all days following inoculation (Figure 3c and e). Therefore, EGFP-neutrophil fluorescence provides a quantifiable measurement of the infection-induced inflammatory response.

Contribution of IL-1α and IL-1β to host defense

IL-1R/MyD88 signaling is an essential immune mechanism required for host defense against *S. aureus* skin infections in mice and humans (Miller *et al.*, 2006; von Bernuth *et al.*, 2008). We previously described that IL-1β (but not IL-1α) has a crucial role in activating IL-1R-mediated cutaneous host defense against an intradermal *S. aureus* challenge in mice (Miller *et al.*, 2007). Thus, we wanted to determine the contribution of IL-1α and IL-1β to IL-1R-mediated cutaneous host defense during the skin wound infection compared with the deeper intradermal infection. Wild-type mice and mice deficient in IL-1R, IL-1α, or IL-1β were inoculated with *S. aureus* either by superficial inoculation of the scalpel wounds or by intradermal injection and lesion sizes, and *in vivo* bioluminescence were evaluated (Figure 4). IL-1R-deficient mice developed up to 3-fold larger lesions and 8- to 15-fold higher bioluminescent signals than wild-type mice (Figure 4a). Similarly, during the deeper intradermal *S. aureus* infection, IL-1R-deficient mice developed 3.7-fold larger lesions and up to 12.8-fold higher bioluminescent signals than wild-type mice (Figure 4b). However, during the superficial infection, mice deficient in either IL-1α or IL-1β had ~1.5-fold larger lesions and up to 3-fold higher bioluminescent signals on days 1 and 3 after inoculation (Figure 4a). Although these increases were statistically significant, they were modest compared with the substantially increased lesion sizes and bioluminescent signals observed in IL-1R-deficient mice. In contrast, for the deeper intradermal infection, IL-1β-deficient mice had lesion sizes and bioluminescent signals that were virtually identical to those of IL-1R-deficient mice, and IL-1α-deficient mice had lesion sizes and bioluminescent signals that closely resembled those of wild-type mice (Figure 4b). Taken together, both IL-1α and IL-1β contributed to IL-1R-mediated host defense during the *S. aureus* skin wound infection, whereas IL-1β was the predominant contributor to IL-1R-mediated host defense during the deeper intradermal *S. aureus* skin infection.

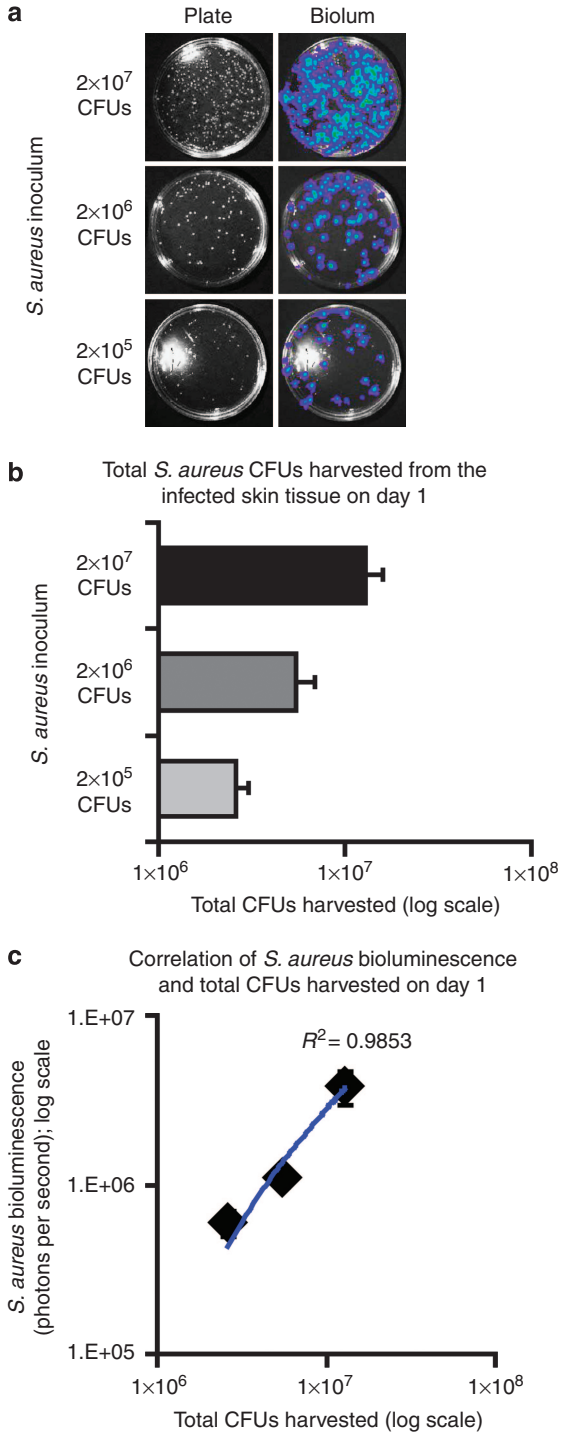

Figure 2. *In vivo* bioluminescence highly correlated with *ex vivo* bacterial colony-forming unit (CFU) counts. Bacteria present within the infected skin lesions that were inoculated with 2×10^5, 2×10^6, and 2×10^7 CFUs per 10 µl of *Staphylococcus aureus* ($n = 5$ mice per group) were harvested from mice on postinoculation day 1 and CFUs were determined after overnight culture. (**a**) Representative bacterial culture plates after overnight culture with or without bioluminescence. (**b**) Mean CFUs of *S. aureus* ± SEM recovered from 8-mm lesional punch biopsies on day 1. (**c**) Correlation between *in vivo* bioluminescence signals and total CFUs harvested from the infected skin lesions. The logarithmic trendline (blue line) and the correlation coefficient of determination (R^2) between *in vivo* bioluminescence signals and total CFUs are shown.

Determination of the *in vivo* efficacy of topical antimicrobial therapy

To determine whether this *S. aureus* skin wound infection model could be used to evaluate the efficacy of topical antimicrobial therapy, we compared the efficacy of the two FDA-approved topical prescription-strength therapies, mupirocin and retapamulin. To perform these studies, we generated a bioluminescent USA300 strain. This strain was used in combination with LysEGFP mice so that both the bacterial burden and infection-induced inflammation could be

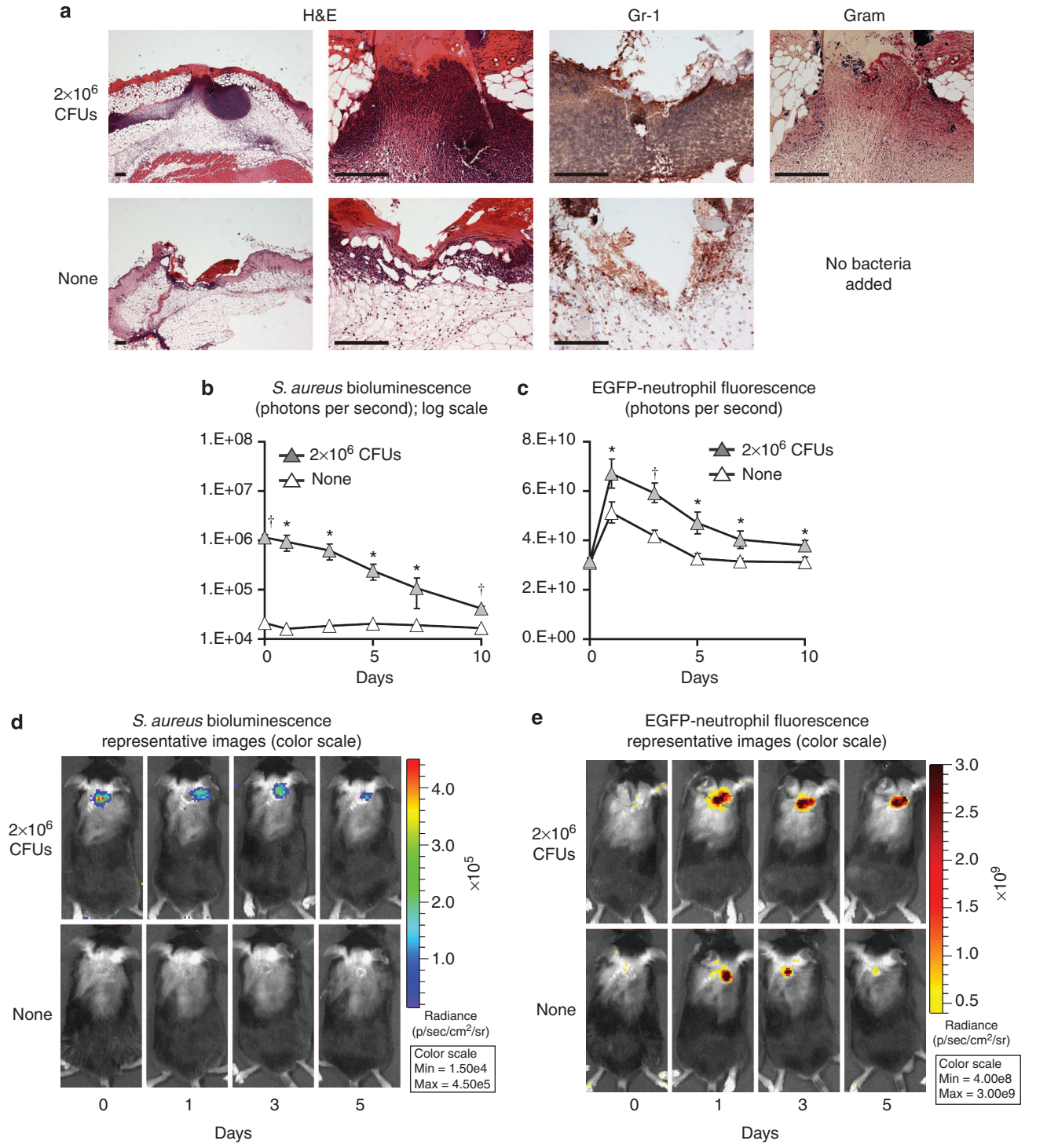

Figure 3. *In vivo* fluorescence imaging to measure the infection-induced inflammation. Three 8-mm in length, parallel scalpel wounds on the backs of (**a**) C57BL/6 mice or (**b**–**e**) LysEGFP mice were inoculated with 2×10^6 colony-forming units (CFUs) per 10 µl of *Staphylococcus aureus* or no bacteria (none). (**a**) Representative photomicrographs (1 of 3, with similar results) of sections from 8-mm punch biopsies taken at 1 day after wounding ± *S. aureus* infection labeled with hematoxylin and eosin (H&E) stain, anti-Gr-1 mAb (neutrophil marker), and Gram stain. Scale bars = 150 µm. (**b**) *In vivo S. aureus* burden as measured by *in vivo* bioluminescence imaging (mean total flux (photons per second) ± SEM) (logarithmic scale). (**c**) Infection-induced inflammation (enhanced green fluorescence protein (EGFP)-neutrophil infiltration) as measured by *in vivo* fluorescence imaging (mean total flux (photons per second) ± SEM). (**d**) Representative photographs of *in vivo S. aureus* bioluminescence. (**e**) Representative photographs of *in vivo* EGFP-neutrophil fluorescence.

measured. Mupirocin 2% ointment, retapamulin 1% ointment, or corresponding vehicle ointments (polyethylene glycol (mupirocin) and white petrolatum (retapamulin)) was topically applied (0.1 ml volume) to the infected skin lesions at 4 hours after inoculation followed by twice-daily (every 12 hours) application for the next 7 days (Figure 5). Mupirocin ointment

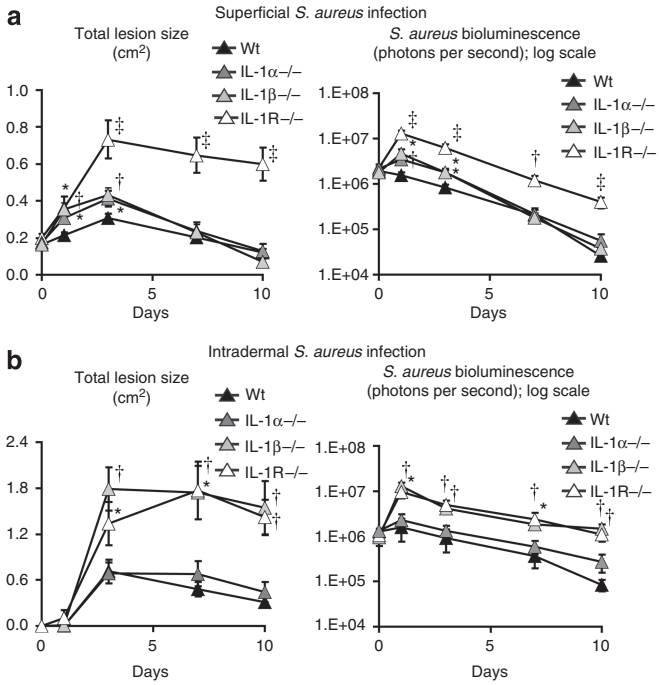

Figure 4. Contribution of IL-1α and IL-1β to IL-1R-mediated host defense against *Staphylococcus aureus* skin infection. IL-1α-, IL-1β-, and IL-1R-deficient mice and wild-type (wt) mice ($n=12$ mice per group) were inoculated with (**a**) 2×10^6 colony-forming units (CFUs) per 10 µl of *S. aureus* in the superficial *S. aureus* skin infection model or with (**b**) an intradermal injection of 2×10^6 CFUs per 100 µl of *S. aureus*. (Left panels) Mean total lesion size (cm^2) ± SEM. (Right panels) *In vivo* bacterial counts as measured by mean total flux (photons per second) ± SEM. $^*P<0.05$; $^\dagger P<0.01$; $^\ddagger P<0.001$, IL-1α-, IL-1β- or IL-1R-deficient mice versus wt mice (Student's *t*-test).

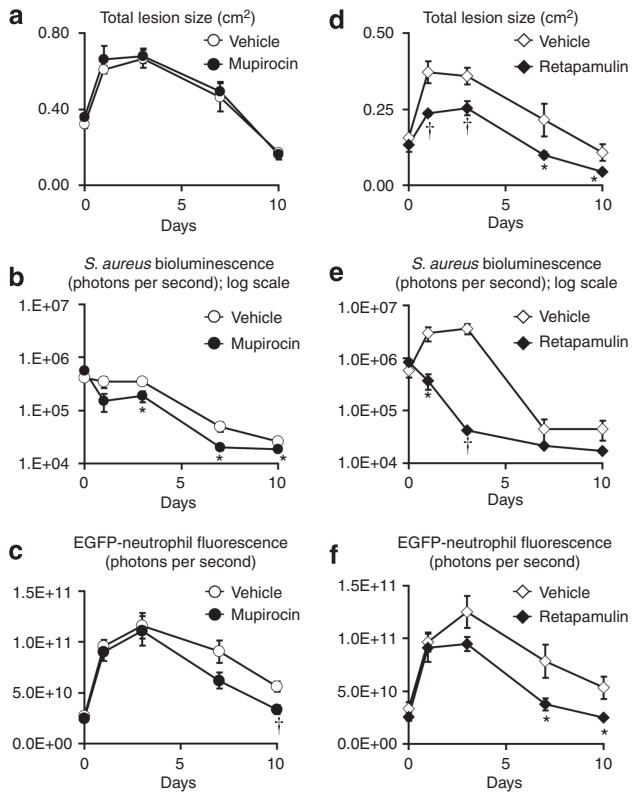

Figure 5. *In vivo* efficacy of mupirocin and retapamulin topical therapy against USA300, a clinically relevant methicillin-resistant *Staphylococcus aureus* (MRSA) strain. Three 8-mm in length, parallel scalpel wounds on the backs of LysEGFP mice were inoculated with 2×10^6 colony-forming units (CFUs) per 10 µl of USA300. (**a**–**c**) Mupirocin 2% ointment, (**d**–**f**) retapamulin 1% ointment, or the corresponding vehicle ointment (polyethylene glycol (mupirocin) and white petrolatum (retapamulin)) ($n=6$ mice per group) were topically applied to the infected skin (0.1 ml volume per treatment) at 4 hours after inoculation followed by twice-daily (every 12 hours) application for the next 7 days. (**a**, **d**) Mean total lesion size (cm^2) ± SEM. (**b**, **e**) Bacterial counts as measured by *in vivo* USA300 bioluminescence (mean total flux (photons per second) ± SEM) (logarithmic scale). (**c**, **f**) Infection-induced inflammation (enhanced green fluorescence protein (EGFP)-neutrophil infiltration) as measured *by in vivo* fluorescence (total flux (photons per second) ± SEM). $^*P<0.05$; $^\dagger P<0.01$; $^\ddagger P<0.001$, antibiotic ointment versus vehicle ointment (Student's *t*-test).

in comparison with vehicle ointment had virtually identical lesion sizes, only slightly lower bioluminescence signals (~2-fold), and a similar degree of inflammation as measured by EGFP-neutrophil fluorescence until day 10, when a 40% decrease was observed (Figure 5a–c). In contrast, retapamulin ointment resulted in a 37–59% decrease in lesion sizes beginning at day 1 after inoculation, an 85-fold reduction in bioluminescent signals by day 3, and in a 24–53% decrease in EGFP-neutrophil fluorescent signals beginning at day 3 compared with vehicle ointment-treated mice (Figure 5d–f). Thus, retapamulin ointment was clinically effective against a USA300 MRSA infection in our *in vivo* model and far superior to mupirocin treatment. An *in vitro* antibiotic sensitivity assay confirmed that this USA300 strain exhibited high resistance against mupirocin, as this strain had a 33,000-fold higher minimal inhibitory concentration of mupirocin compared with a mupirocin-sensitive MSSA (methicillin-sensitive *S. aureus*) strain (SH1000) (625 vs. 0.002 µg l^{-1}, respectively). Taken together, these results demonstrate that this wound infection model can be used to determine the *in vivo* effectiveness of topical therapy against a clinically relevant MRSA USA300 strain, which will be critical in the future evaluation of other candidate antimicrobial therapies.

It should be mentioned that the bioluminescent construct in this USA300 strain was stable at early time points *in vivo*, as 100% of the *ex vivo* CFUs maintained this construct at least through day 3 (data not shown), suggesting that the *in vivo* bioluminescence signals closely approximated the actual bacterial burden at the time points when we observed major differences (days 1–3). However, at days 7 and 10, 76 and 50% of *ex vivo* CFUs maintained the construct, suggesting that at these late time points the *in vivo* bioluminescence signals may underestimate the actual bacterial burden.

DISCUSSION

Skin infections caused by *S. aureus* and MRSA have emerged as a major public health threat in the United States (McCaig *et al.*, 2006; Moran *et al.*, 2006). As new and effective

treatment strategies are needed, a rapid and cost-effective preclinical animal model is necessary to investigate *in vivo* protective immune responses and the efficacy of potential therapeutics. In this study a mouse model of a *S. aureus* skin wound infection was developed in which a bioluminescent *S. aureus* or CA-MRSA strain was inoculated into skin wounds and *in vivo* bioluminescence and fluorescence imaging was used to noninvasively track the bacterial burden and infection-induced inflammation in real-time. Using this model, we uncovered a key role for IL-1α (in addition to IL-1β) in the cutaneous immune response *in vivo*. Importantly, this model was successfully used to evaluate the efficacy of topical antibiotic therapy against the clinically relevant CA-MRSA strain USA300.

In this study, we found that both IL-1α and IL-1β contributed to host defense during a *S. aureus* skin wound infection, whereas IL-1β was more critical during a deeper intradermal *S. aureus* skin infection. A recent study demonstrated that keratinocytes stimulated with *S. aureus* lipoteichoic acid and peptidoglycan triggered an autocrine IL-1α signaling loop, which resulted in continuous production of neutrophil chemokines (Olaru and Jensen, 2010). In addition, keratinocytes constitutively express prestores of IL-1α that are released after nonspecific inflammation or infection (Lee *et al.*, 1997). Thus, the important role for IL-1α during the skin wound infection is likely because of the release of the IL-1α from keratinocytes. In contrast, during the intradermal infection, the inducible IL-1β response of the bone-marrow-derived recruited cells of the abscess was a more critical determinant for host defense (Miller *et al.*, 2007). Taken together, these results suggest that keratinocytes (and IL-1α) have a greater role in the cutaneous immune response during a *S. aureus* skin wound infection. Future studies will use this model to investigate other important cutaneous host defense mechanisms, including the role of pattern recognition receptors (e.g., Toll-like receptors), cytokine and chemokine responses, and antimicrobial peptides.

As this model represented a *S. aureus* infection of open skin wounds, it provided the opportunity to evaluate the efficacy of topical antimicrobial therapy. We evaluated the two FDA-approved prescription-strength topical ointments, mupirocin and retapamulin, against the clinically relevant USA300 CA-MRSA strain. We found that mupirocin ointment provided minimal antimicrobial activity against this USA300 strain, which we confirmed had high *in vitro* resistance to mupirocin. In contrast, retapamulin 1% ointment substantially reduced the bacterial burden by day 3 (85-fold), dramatically decreased the infection-induced inflammation (>50%), and had markedly smaller lesions that healed at a faster rate. These findings have clear clinical relevance and demonstrate how the presence of antibiotic resistance can complicate treatment. As retapamulin was clinically effective in eradicating *S. aureus* infection *in vivo*, these results suggest that retapamulin could serve as an alternative topical agent to help treat *S. aureus*/MRSA skin infections (and perhaps against nasal colonization), especially given the growing incidence of mupirocin resistance. Last, when comparing the vehicle ointments, white petrolatum, the vehicle for retapamulin, enhanced the bacterial burden (Figure 5e), which was not observed with polyethylene glycol, the vehicle for mupirocin (Figure 5b). Therefore, the vehicle may also be an important determinant for the development of future topical antibiotic therapies.

It should be mentioned that we did not observe a major difference in virulence with the USA300 strain compared with the laboratory SH1000 strain in this mouse model. The reason for this is likely because of differences in susceptibility between human and mouse cells to cytolytic toxins produced by USA300 (Diep *et al.*, 2010). One example is PVL, which lyses human and rabbit neutrophils (but not mouse neutrophils), and has been demonstrated to have a critical role in necrotizing pneumonia in rabbits but not in mice (Bubeck *et al.*, 2008; Diep *et al.*, 2010). In addition, PVL has been shown not to be a virulence determinant for skin infections in mice (Bubeck *et al.*, 2008). Thus, in certain instances regarding species-specific virulence factors, the use of a mouse model has some limitations.

Taken together, the mouse model developed in this study utilized noninvasive *in vivo* bioluminescence and fluorescence imaging to determine the bacterial burden and infection-induced inflammation without the need for euthanasia. Thus, the use of this model will substantially decrease animal usage, an important consideration for animal protection. This model could be used to study mechanisms of protective cutaneous immune responses and as a preclinical animal model to investigate and compare the *in vivo* efficacy of new topical (or perhaps systemic) antimicrobial therapeutic strategies.

MATERIALS AND METHODS

S. aureus bioluminescent strains

The bioluminescent *S. aureus* SH1000 strain, ALC2906, which possesses the shuttle plasmid pSK236 with the *pbp2* (*penicillin-binding protein 2*) promoter fused to the *luxABCDE* cassette from *Photorhabdus luminescens*, was used as previously described (Miller *et al.*, 2006). This strain emits bioluminescent signals from live bacteria in all stages of the *S. aureus* life cycle. The bioluminescent MRSA strain, ALC6668, was generated from a clinical USA300 isolate (Stemper *et al.*, 2006) in the same fashion as ALC2906.

Preparation of *S. aureus* for skin inoculation

S. aureus bioluminescent strains ALC2906 and ALC6668 were prepared as described (Cho *et al.*, 2010). Briefly, mid-logarithmic phase bacteria were obtained after a 2-hour subculture of a 1:50 dilution of the overnight culture. Bacterial cells were washed twice and resuspended in sterile pharmacy grade saline (0.9%) at the indicated concentrations. CFUs were verified after overnight culture of plates.

Mice

Male mice, 6–8 weeks old, on a C57BL/6 genetic background were used in all experiments. C57BL/6 wild-type mice and IL-1R-deficient mice (B6.129S7-*Il1r1*^{tm1Imx}/J) were obtained from Jackson Laboratories, Bar Harbor, ME. In some experiments, LysEGFP mice, which is a mouse strain that possesses green fluorescent myeloid cells because of a knock-in of EGFP into the lysozyme M gene, were used (Faust *et al.*, 2000).

Mouse model of *S. aureus* skin wound infection

All procedures were approved by the University of California Los Angeles Chancellor's animal research committee. The skin of mice on the posterior upper back and neck was shaved, and three parallel 8-mm in length full-thickness scalpel cuts (no. 11 blade) were made into the dermis. The wounds were inoculated with 10 µl of *S. aureus* strain ALC2906 (2×10^5, 2×10^6, or 2×10^7 CFUs per 10 µl) or ALC6668 (2×10^6 CFUs per 10 µl) with a micropipettor. Control uninfected mice were given a sham inoculation with 10 µl of saline alone. Measurements of total lesion size (cm^2) were made by analyzing digital photographs using the software program "Image J" (NIH Research Services Branch; http://rsbweb.nih.gov/ij/) and a millimeter ruler as a reference. In some experiments, a deeper *S. aureus* infection was generated by inoculating the backs of mice with an intradermal injection of *S. aureus* SH1000 strain (2×10^6 CFUs per 100 µl) in sterile pharmacy-grade saline (0.9%) using a 27-gauge insulin syringe (Cho *et al.*, 2010).

Quantification of *in vivo S. aureus* (*in vivo* bioluminescence and CFUs)

Mice were anesthetized via inhalation of isoflurane (2%) and *in vivo* bioluminescence imaging was performed using the Xenogen IVIS imaging system (Caliper Life Sciences) as previously described (Cho *et al.*, 2010). Data are presented on color scale overlaid on a grayscale photograph of mice and quantified as total flux (photons per second) within a circular region of interest (1×10^3 pixels) using Living Image software (Xenogen). In some experiments, to confirm that the *in vivo* bioluminescence signals accurately represented the bacterial burden *in vivo*, *S. aureus* CFUs were determined after overnight cultures of homogenized (Pro200 Series homogenizer (Pro Scientific, Oxford, CT)) 8-mm punch biopsy (Acuderm, Fort Lauderdale, FL) specimens of lesional skin taken at day 1 after inoculation.

Histological analysis

Mice were euthanized and lesional 8-mm punch biopsy (Acuderm) skin specimens were bisected and one half was fixed in formalin (10%) and embedded in paraffin and the other half was embedded in Tissue-Tek O.C.T. (optimal cutting temperature) compound (Sakura Finetek, Torrance, CA) and frozen in liquid nitrogen. Paraffin sections (4 µm thick) were cut and stained with hematoxylin and eosin and Gram stain. Frozen sections (4 µm thickness) were cut and were then labeled with a biotinylated rat anti-mouse Gr-1 mAb (1 µg ml^{-1}; clone RB6-8C5; IgG2b isotype; BD Pharmingen, San Diego, CA) or isotype control mAb using the immunoperoxidase method as previously described (Cho *et al.*, 2010).

Quantification of neutrophil recruitment to the site of *S. aureus* skin wound infection (*in vivo* fluorescence imaging)

To obtain a measurement of neutrophil infiltration, LysEGFP mice were used. After *in vivo* bioluminescence imaging, *in vivo* fluorescence imaging was performed by using the Xenogen IVIS (Caliper Life Sciences). EGFP-expressing cells were visualized using the GFP filter for excitation (445–490 nm) and emission (515–575 nm) at an exposure time of 0.5 seconds (Kim *et al.*, 2008, 2009). Data are presented on color scale overlaid on a grayscale photograph of mice and quantified as total flux (photons per second) within a circular region of interest (1×10^3 pixels) using Living Image software (Xenogen).

Administration of topical mupirocin and retapamulin ointment

The infected skin wounds were treated topically by applying 0.1 ml of mupirocin 2% ointment (Bactroban; GlaxoSmithKline, Research Triangle Park, NC), retapamulin 1% ointment (Altabax; Stiefel/GlaxoSmithKline), or the corresponding vehicle ointment (polyethylene glycol (mupirocin) and white petrolatum (retapamulin)) at 4 hours after *S. aureus* inoculation followed by twice-daily (every 12 hours) application thereafter for a total of 7 days.

Statistical analysis

Data were compared using Student's *t*-test (two tailed). All data are expressed as mean ± SEM. Values of $P < 0.05$ were considered statistically significant.

CONFLICT OF INTEREST

The authors state no conflict of interest.

ACKNOWLEDGMENTS

This work was supported in part by grants R01 AI078910 and R03 AR054534 (to LSM), R01 AI059091 (to JK), T32 AR058921 (to JSC), and the UCLA Small Animal Imaging Resource Program (SAIRP) R24 CA92865 from the National Institutes of Health and the Dermatologic Research Foundation of California (to JZ).

REFERENCES

Bode LG, Kluytmans JA, Wertheim HF *et al.* (2010) Preventing surgical-site infections in nasal carriers of *Staphylococcus aureus*. *N Engl J Med* 362:9–17

Boucher HW, Corey GR (2008) Epidemiology of methicillin-resistant *Staphylococcus aureus*. *Clin Infect Dis* 46(Suppl 5):S344–9

Bubeck WJ, Palazzolo-Ballance AM, Otto M *et al.* (2008) Panton-Valentine leukocidin is not a virulence determinant in murine models of community-associated methicillin-resistant *Staphylococcus aureus* disease. *J Infect Dis* 198:1166–70

Cho JS, Pietras EM, Garcia NC *et al.* (2010) IL-17 is essential for host defense against cutaneous *Staphylococcus aureus* infection in mice. *J Clin Invest* 120:1762–73

Daum RS (2007) Clinical practice. Skin and soft-tissue infections caused by methicillin-resistant Staphylococcus aureus. *N Engl J Med* 357:380–90

David MZ, Daum RS (2010) Community-associated methicillin-resistant *Staphylococcus aureus*: epidemiology and clinical consequences of an emerging epidemic. *Clin Microbiol Rev* 23:616–87

Deleo FR, Chambers HF (2009) Reemergence of antibiotic-resistant *Staphylococcus aureus* in the genomics era. *J Clin Invest* 119:2464–74

Diep BA, Chan L, Tattevin P *et al.* (2010) Polymorphonuclear leukocytes mediate *Staphylococcus aureus* Panton-Valentine leukocidin-induced lung inflammation and injury. *Proc Natl Acad Sci USA* 107:5587–92

Elston DM (2007) Community-acquired methicillin-resistant *Staphylococcus aureus*. *J Am Acad Dermatol* 56:1–16

Faust N, Varas F, Kelly LM *et al.* (2000) Insertion of enhanced green fluorescent protein into the lysozyme gene creates mice with green fluorescent granulocytes and macrophages. *Blood* 96:719–26

Hahn BL, Onunkwo CC, Watts CJ *et al.* (2009) Systemic dissemination and cutaneous damage in a mouse model of staphylococcal skin infections. *Microb Pathog* 47:16–23

Heggers JP, McHugh T, Zoellner S *et al.* (1989) Therapeutic efficacy of timentin and augmentin versus silvadene in burn wound infections. *J Burn Care Rehabil* 10:421–4

Holland DB, Bojar RA, Jeremy AH *et al.* (2008) Microbial colonization of an *in vitro* model of a tissue engineered human skin equivalent—a novel approach. *FEMS Microbiol Lett* 279:110–5

Jones RN, Nilius AM, Akinlade BK *et al.* (2007) Molecular characterization of *Staphylococcus aureus* isolates from a 2005 clinical trial of uncomplicated skin and skin structure infections. *Antimicrob Agents Chemother* 51:3381–4

Kennedy AD, Bubeck WJ, Gardner DJ *et al.* (2010) Targeting of alpha-hemolysin by active or passive immunization decreases severity of USA300 skin infection in a mouse model. *J Infect Dis* 202:1050–8

Kim MH, Curry FR, Simon SI (2009) Dynamics of neutrophil extravasation and vascular permeability are uncoupled during aseptic cutaneous wounding. *Am J Physiol Cell Physiol* 296:C848–56

Kim MH, Liu W, Borjesson DL *et al.* (2008) Dynamics of neutrophil infiltration during cutaneous wound healing and infection using fluorescence imaging. *J Invest Dermatol* 128:1812–20

King MD, Humphrey BJ, Wang YF *et al.* (2006) Emergence of community-acquired methicillin-resistant *Staphylococcus aureus* USA 300 clone as the predominant cause of skin and soft-tissue infections. *Ann Intern Med* 144:309–17

Kugelberg E, Norstrom T, Petersen TK *et al.* (2005) Establishment of a superficial skin infection model in mice by using *Staphylococcus aureus* and *Streptococcus pyogenes*. *Antimicrob Agents Chemother* 49:3435–41

Lee RT, Briggs WH, Cheng GC *et al.* (1997) Mechanical deformation promotes secretion of IL-1 alpha and IL-1 receptor antagonist. *J Immunol* 159:5084–8

McCaig LF, McDonald LC, Mandal S *et al.* (2006) *Staphylococcus aureus*-associated skin and soft tissue infections in ambulatory care. *Emerg Infect Dis* 12:1715–23 http://www.cdc.gov/ncidod/EID/vol12no11/06-0190.htm

McRipley RJ, Whitney RR (1976) Characterization and quantitation of experimental surgical-wound infections used to evaluate topical antibacterial agents. *Antimicrob Agents Chemother* 10:38–44

Miller LS, O'Connell RM, Gutierrez MA. *et al.* (2006) MyD88 mediates neutrophil recruitment initiated by IL-1R but not TLR2 activation in immunity against *Staphylococcus aureus*. *Immunity* 24:79–91

Miller LS, Pietras EM, Uricchio LH *et al.* (2007) Inflammasome-mediated production of IL-1beta is required for neutrophil recruitment against *Staphylococcus aureus in vivo*. *J Immunol* 179:6933–42

Molne L, Verdrengh M, Tarkowski A (2000) Role of neutrophil leukocytes in cutaneous infection caused by *Staphylococcus aureus*. *Infect Immun* 68:6162–7

Moran GJ, Krishnadasan A, Gorwitz RJ *et al.* (2006) Methicillin-resistant S. aureus infections among patients in the emergency department. *N Engl J Med* 355:666–74

Olaru F, Jensen LE (2010) *Staphylococcus aureus* stimulates neutrophil targeting chemokine expression in keratinocytes through an autocrine IL-1alpha signaling loop. *J Invest Dermatol* 130:1866–76

Rittenhouse S, Singley C, Hoover J *et al.* (2006) Use of the surgical wound infection model to determine the efficacious dosing regimen of retapamulin, a novel topical antibiotic. *Antimicrob Agents Chemother* 50:3886–8

Rode H, de Wet PM, Millar AJ *et al.* (1988) Bactericidal efficacy of mupirocin in multi-antibiotic resistant *Staphylococcus aureus* burn wound infection. *J Antimicrob Chemother* 21:589–95

Stemper ME, Brady JM, Qutaishat SS *et al.* (2006) Shift in *Staphylococcus aureus* clone linked to an infected tattoo. *Emerg Infect Dis* 12:1444–6

Tenover FC, Goering RV (2009) Methicillin-resistant *Staphylococcus aureus* strain USA300: origin and epidemiology. *J Antimicrob Chemother* 64:441–6

Thomas CM, Hothersall J, Willis CL *et al.* (2010) Resistance to and synthesis of the antibiotic mupirocin. *Nat Rev Microbiol* 8:281–9

Verdrengh M, Tarkowski A (1997) Role of neutrophils in experimental septicemia and septic arthritis induced by *Staphylococcus aureus*. *Infect Immun* 65:2517–21

von Bernuth H, Picard C, Jin Z *et al.* (2008) Pyogenic bacterial infections in humans with MyD88 deficiency. *Science* 321:691–6

Wang R, Braughton KR, Kretschmer D *et al.* (2007) Identification of novel cytolytic peptides as key virulence determinants for community-associated MRSA. *Nat Med* 13:1510–4

Yang LP, Keam SJ (2008) Retapamulin: a review of its use in the management of impetigo and other uncomplicated superficial skin infections. *Drugs* 68:855–73